Synergism between α-amino acid-derived polyamidoamines and sodium montmorillonite for enhancing the flame retardancy of cotton fabrics

Alessandro Beduini[1], Federico Carosio[2], Paolo Ferruti[1], Elisabetta Ranucci[1], Jenny Alongi[1*]

[1]Dipartimento di Chimica, Università degli Studi di Milano, Via C. Golgi 19, 20133 Milan, Italy.

[2]Dipartimento di Scienza Applicata e Tecnologia, Politecnico di Torino, Alessandria campus, Via T. Micheal, 15121 Alessandria, Italy.

* Correspondence: jenny.alongi@unimi.it; Tel.: +39 0250314108

Abstract

Polyamidoamine (PAA)/sodium montmorillonite (MMT) nanocomposite coatings were investigated as flame retardants for cotton to ascertain whether the addition of clay improved the efficacy of PAAs thanks to its ability to act as insulating shield during combustion. Three amphoteric PAAs were obtained by reacting *N,N'*-methylenebisacrylamide with natural α-amino acids, namely glycine (M-GLY), arginine (M-ARG) and glutamic acid (M-GLU). These PAAs act as intumescent flame retardants for cotton performing well in horizontal flame spread tests (HFSTs) but failing to inhibit combustion in vertical flame spread tests (VFSTs). All three PAAs have been proven to form strong interactions in water with MMT via their protonated tert-amine groups. The presence of 12.5% MMT did not significantly change the thermal and thermo-oxidative stability of PAA coatings, while 2% MMT add-on affected those of both untreated and PAA-treated cotton fabrics. In HFSTs, substituting 2% MMT for PAA did not significantly change the flame retardant efficacy of the coatings. In VFSTs, the 2% MMT/14% PAA combination inhibited cotton ignition, regardless of the PAA structure, while in the 2% MMT/11% PAA combination M-GLU protected cotton from ignition, M-ARG extinguished the flame and M-GLY burned completely. By further reducing the PAA content to 8%, only M-GLU quenched cotton combustion, leaving an RMF of 82%. The fact that neither MMT nor PAAs alone induced flame extinguishment at the same add-ons used in the adopted formulations suggests a synergistic behavior of MMT and PAAs.

Keywords: polyamidoamines; MMT; flame retardancy; cotton; nanocomposite coatings.

1. Introduction

Flame retardants (FRs) for textiles have been studied since the 1950s. Due to the numerous fields of application of textiles, including protective garments, automotive, transportations, they are still of industrial relevance. FRs for cotton have been the most widely investigated [1-7].

Inorganic nanoparticles have emerged as promising flame retardant candidates, especially when applied as coating on textiles [8,9]. One of their advantages, compared to traditional FRs, is the small amount of material required to effectively coat the fabrics and exert their function. In addition, they can be applied using different deposition procedures, including nanoparticle adsorption, in situ synthesis of nanoparticles through sol-gel process [10-15], and Layer-by-Layer (LbL) deposition [16-19]. The mechanism of action of flame retardant nanocomposite coatings, as in bulk nanocomposites, is based on the accumulation, during the combustion process and consequent overheating of textile, of nanoparticles on the coating surface, forming an inorganic barrier that protects the underlying polymer and favors char formation [20-23]. Montmorillonite (MMT), a multilayered aluminosilicate clay bearing sodium or calcium ions in the interlaminar space, is a widely used nanosized inorganic filler present in the flame retardant formulations for polymers. During burning, MMT produces an SiO_2 covering, which plays a dual role of insulating and shielding the polymer. This barrier prevents heat, oxygen, and mass transfer, altering the degradation pathways of polymers, and limiting the mobility of polymer chains [24,25]. MMT can help to reduce heat release, smoke release, and the rate of production of toxic gases from composites during burning [26-28].

To achieve satisfactory flame retardant efficiency, MMT and organically modified MMT are normally combined with several conventional FRs, including halogenated compounds, metal hydroxides, and P-containing compounds [27]. This combination turned out be successful particularly for thermoplastics since the addition of layered silicate prevents polymer melt dripping during burning hence fire spreading. In these cases, the synergism between MMT and the FR has been proposed. However, synergy is not always established between MMT and FRs. The possibility of synergism, antagonism or simply cooperation taking place depends on the configuration of the combustion test, as observed in polypropylene/MMT nanocomposites [28,29] and on the concentration of MMT, as found in polyamide 6/MMT nanocomposites [30].

In the last decades, academic and industrial research efforts have been focused on the development of non-toxic flame retardant formulations, and different bio-based compounds have been investigated as “green” flame retardant additives with good char-forming ability [31]. In this context, polyamidoamines (PAAs) may represent a new family of “green” polymeric FRs for cotton. PAAs are synthetic, biocompatible, and degradable polymers synthesized by the aza-Michael polyaddition of primary amines or secondary diamines to bisacrylamides [32-34]. PAA synthesis takes place in water, at room temperature, without adding catalysts and releasing by-products; therefore, PAA preparation can be considered “green” and easily scalable. Many PAAs were studied as flame retardants for cotton fabrics [35,36]. In particular, the PAAs deriving from the polyaddition of *N,N’*-methylenebisacrylamide with different natural α-amino acids turned to be particularly effective [37].

These PAAs extinguished the flame in Horizontal Flame Spread Tests (HFSTs) but failed to suppress the flame in the more drastic Vertical Flame Spread Tests (VFSTs), even at add-ons of 20% or more. Nevertheless, the PAA obtained from the polyaddition of L-cystine with *N,N'*-methylenebisacrylamide (M-CYSS) was proven to extinguish the flame in VFSTs at 16% add-on [38], probably due to its ability to capture radicals present in the gas phase. However, its performance in HFSTs was significantly less efficient than other previously tested non-sulfur PAAs.

In previous work, an amphoteric, predominantly cationic PAA bearing one guanidine residue per repeating unit was shown to form stable ionic interactions in aqueous media with MMT and, in cross-linked form, to form composite hydrogels with it [39]. On the other hand, all α-amino acid-derived PAAs are amphoteric and present a pH-dependent ionic species distribution [40]. At pH 4.5, at which PAAs are deposited onto cotton, they bear approximately 100% protonated tert-amine groups in the backbone, while the carboxylate pendants are negatively charged. It can therefore be assumed that they too can create strong interactions with MMT. The aim of this work is to demonstrate the occurrence of strong ionic interactions between α-amino acid-derive PAA flame retardants and MMT, to study the effect of these interactions on the thermal-oxidative stability of cotton fabrics and verify if their combination can give rise to a synergistic effect in terms of flame retardancy.

2. Experimental part

2.1 Materials

N,N'-methylenebisacrylamide (M, 99%), L-glutamic acid (GLU, 99%), glycine (GLY, 99%), L-arginine (ARG, 99%), lithium hydroxide monohydrate ($LiOH \cdot H_2O$, 98%), 1M HCl, were supplied by Sigma-Aldrich (Milan, Italy) and sodium montmorillonite (MMT) by BYK additives Inc. (Texas, USA). Cotton (COT) with an area density of 240 $g \cdot m^{-2}$ was purchased from Fratelli Ballesio S.r.l. (Turin, Italy).

2.2 Synthesis of polyamidoamines

Synthesis of M-GLY. M-GLY was synthesized following a previously reported procedure [35]. In brief, M (4.00 g, 25.94 mmol), glycine (1.95 g, 25.94 mmol) and $LiOH \cdot H_2O$ (1.11 g, 25.94 mmol) were dispersed in H_2O (11 mL) and heated under stirring up to 45 °C until complete dissolution of all monomers. The reaction mixture was then maintained at 25 °C for 5 days in the dark. After this time, it was diluted to 70 mL with water, and the pH adjusted to 4.00 with 1 M HCl. The final product was retrieved by freeze-drying. The yield was nearly quantitative.

M-ARG and *M-GLU* were synthesized following the same procedure described for M-GLY, using the following amounts of the reagents [35,37]. M-ARG: M (4.00 g, 25.94 mmol), and L-arginine (4.52 g, 25.94 mmol), dissolved in H_2O (13 mL); reaction time 10 days. M-GLU: M (4.00 g, 25.94 mmol), L-glutamic acid (3.82 g, 25.94 mmol), and lithium hydroxide monohydrate (2.22 g, 51.88 mmol) dissolved in H_2O (5 mL), reaction time 10 days.

2.3 Study of MMT/polyamidoamine interactions

MMT (0.10 g) was suspended in 10 mL water under stirring for 24 h. Then, a PAA solution (0.70 g in 10 ML water) was added to the MMT suspension and kept under stirring for 0.5 h. At the end, the suspension containing MMT/PAA system was freeze-dried.

2.4 Treatment of cotton fabrics with MMT/PAAs

Strips of cotton fabrics 30 mm x 60 mm in size were initially dried at 100 °C for 4 min and then weighed. In parallel, a 1.0 wt.% MMT suspension was prepared dispersing MMT in water and maintaining for 24 h under stirring. Subsequently, cotton fabrics were sprayed with the MMT suspension (2 x 10 mL), and then dried at 100 °C for 4 min. After this time, the specimens were impregnated twice with PAA aqueous solutions of suitable concentration, drying at 100 °C for 4 min after each deposition. The total dry solid add-ons (*Add-on, wt.-%*) were determined weighing each sample before (W_i) and after (W_f) the impregnation step. The add-ons were calculated using Equation (1):

$$Add - on = \frac{W_f - W_i}{W_i} \times 100 \qquad (1)$$

The concentrations of the impregnating PAA solutions were 7.0 wt.% for reaching 14% add-on, 5.0 wt.% for reaching 11% add-on, and 4.0 wt.% for reaching 8% add-on. The MMT add-on adopted was 2% in all experiments. Treated-cotton fabrics were coded as the following example: COT/MMT/M-GLY, which is the code for a cotton sample treated with 2% add-on sodium montmorillonite and 14% add-on M-GLY.

2.5 Characterization techniques

Thermogravimetric analyses (TGA) of PAAs and PAA-treated cotton fabrics (5 mg in open alumina crucibles) were performed in inert (nitrogen) and oxidative (air) atmosphere using a TAQ500 thermogravimetric balance (TA Waters, Milan, Italy) from 50 to 800 °C, heating rate 10 °C min^{-1}, 20 mL min^{-1} gas flow.

The surface of untreated and PAA-treated cotton fabrics was analyzed by an EVO 15 equipped with a ULTIM MAX 40 probe scanning electron microscope (SEM) manufactured by Zeiss (Ramsey, NJ,

136 USA) and operating at 8.5 mm working distance, under 5 kV beam voltage. A fabric piece (5 mm ×
137 5 mm) was fixed to a sample holder and then gold-metallized; the instrument was equipped with
138 Energy-Dispersive X-ray Spectroscopy probe (EDX, Jena, Germany) for elemental analysis.
139 X-ray diffraction spectra of MMT and MMT/PAAs were recorded using a Miniflex 600
140 diffractometer (Rigaku Europe SE, Germany) under 40 kV voltage, 15 mA current, with Cu
141 $K_{\alpha 1}$ radiation at 1.5405 Å.
142
143 *2.6 Combustion tests of MMT/PAA-treated cotton fabrics*
144 Horizontal flame spread tests (HFSTs) and Vertical flame spread tests (VFSTs) were carried out by
145 applying a 20 ± 5 mm long butane flame to the short side of 30 mm × 60 mm specimens according
146 to the ISO 3795 [41] and ISO 15025 [42] standards modified in terms of cotton size specimens and
147 flame application time. In the horizontal configuration the sample was positioned in a metallic frame
148 tilted at an angle of 45° along its longer axis and then ignited for 3 s. In the vertical configuration, the
149 butane flame was applied for 2 s on the center of the short side of the specimens. All combustion tests
150 were tripled and the combustion and afterglow time (s) and residual mass fraction (RMF, %) were
151 determined. Limiting oxygen index (LOI) tests were performed with a Ceast Fire apparatus (Turin,
152 Italy) according to the ISO 4589 standard [43].
153 The resistance to a 35 $kW \cdot m^{-2}$ irradiative heat flux of square fabric samples (100 mm × 100 mm) was
154 investigated using an oxygen-consuming cone calorimeter (Nose-lab ATS advanced, Milan, Italy).
155 Measurements were carried out in horizontal configuration following a procedure previously reported
156 [44], optimized based on the ISO5660 standard [45]. Parameters such as the time to ignition (TTI, s),
157 peak of heat release rate (pkHRR, $kW \cdot m^{-2}$), total heat release (THR, $MJ \cdot m^{-2}$), and residual mass
158 fraction (RMF, wt.%) were determined. Prior to the combustion tests, all specimens were conditioned
159 to constant weight at 23 ± 1 °C for 48 h at 50% relative humidity in a climatic chamber. Each
160 experiment was performed in triplicate and the mean standard deviation calculated.
161
162 *2.7 Whiteness index measurements of MMT/PAA-treated cotton fabrics*
163 The whiteness index (WI) is a dimensionless parameter depending on the color saturation and
164 lightness of the sample, which ranges from 0 to 120 and indicates how white a sample is, the higher
165 the value the whiter the sample.

166 $$WI = 100 - \sqrt{(100 - L)^2 + + a^2 + b^2} \qquad \text{Eq. 1}$$

167 where L indicates the sample brightness, a and b are chromaticity coordinates. The whiteness index
168 of untreated and MMT-, PAA- and MMT/PAA-treated cotton samples was measured following the

ISO 2469 standard [46], using the SA0835/OWM SAMA whiteness meter (SAMA Tools, Viareggio, Italy). For each sample, measurements were performed in triplicate, and the resulting WI value was obtained as the average of three measurements.

2.8 Tensile tests of MMT/PAA-treated cotton fabrics

Tensile tests were performed on cotton specimens 100 mm x 15 mm in length according to the ISO13934 standard [47]. Analyses were performed using an Instron 5966 (Instron, High Wycombe, UK) instrument equipped with wave clamps; setting: 10 mm·min^{-1} strain rate, and 2 N preload.

3. Results and discussion

3.1 Rationale

In a previous work, the ability of an amphoteric and predominantly cationic polyamidoamine named AGMA1 to give rise to strong interactions with MMT was demonstrated [39]. These interactions were ascribed to the exchange reaction between the protonated guanidine pendants and protonated tert-amines present in AGMA1 repeat units with the sodium cations placed in the interlayer space of MMT. The aim of this work is to investigate whether differently charged amphoteric α-amino acid-derived PAAs, namely M-GLY, M-ARG and M-GLU (Figure 1) can give rise to equally strong interactions with MMT (Figure 2), forming nanocomposite layers that improve the thermal-oxidative stability and combustion resistance of cotton fabrics.

The pH-dependent speciation curves of M-GLY [35], M-ARG [35] and M-GLU were obtained from the pK_a values of the ionizable groups present in their repeat units (Table 1), following the procedure described in the Supplementary Materials (Figures S1 and S2 in Supplementary Materials). Isoelectric point (IP) values are consistent with a slight net positive charge per M-GLY repeat unit (+0.005), a high net positive charge per M-ARG repeat unit (+1.02), and a negative charge per M- GLU repeat unit (-0.35) at pH 4.0.

Table 1. pK_a values, IP and net charge values of PAAs' repeat units.

Repeat Unit	pK_a values	IP	Net charge at pH 4
M-GLY [a]	$pK_{a\text{-}COOH}$ = 1.90 $pK_{a\text{-}NR3}$ = 7.70	4.8	+0.005
M-ARG [b]	$pK_{a\text{-}COOH}$ = 2.2 $pK_{a\text{-}NR3}$ = 6.4 $pK_{a\text{-}guanidine}$ > 10	9.7	+1.02
M-GLU [c]	$pK_{a\text{-}COOH}$ = 2.32 $pK_{a\text{-}COOH}$ = 4.28 $pK_{a\text{-}NR3}$ = 7.78	3.3	-0.35

[a] and [b] Data from [35]. [c] See Figures S1 and S2 in Supplementary Materials.

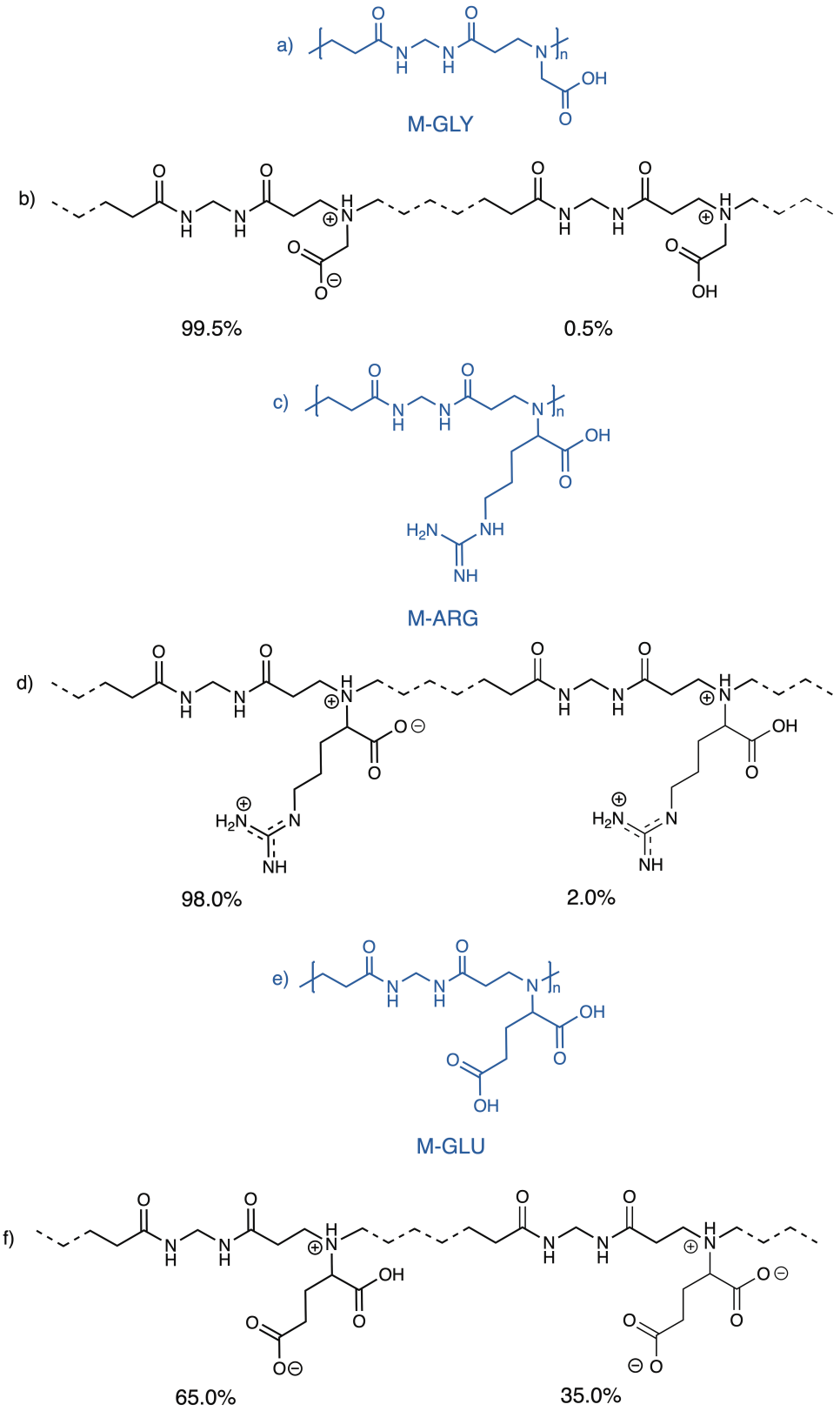

Figure 1. Repeat units of: M-GLY (**a**), M-ARG (**c**) and M-GLU (**e**).
Ionic species distribution at pH 4.0 for: M-GLY (**b**), M-ARG (**d**) and M-GLU (**f**).

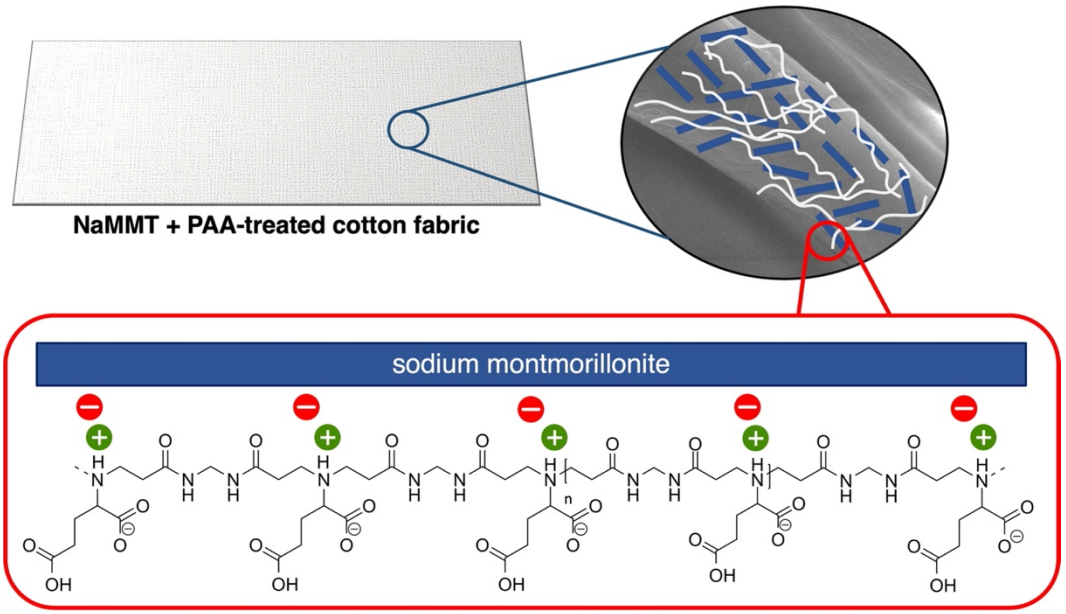

Figure 2. Scheme of interactions occurring between PAAs and sodium montmorillonite on cotton fabrics. The structure of M-GLU is shown as an example.

198 *3.2 Synthesis of PAAs*

199 M-GLY, M-ARG and M-GLU were prepared by the aza-Michael polyaddition of *N,N'*-
200 methylenebisacrilamide (M) with the α-amino acids glycine, L-arginine and L-glutamic acid
201 following a previously reported procedure (Scheme 1) [37]. They were obtained in a single step in
202 water at pH 11 and solid concentrations from 40 to 50 wt.%. They were retrieved by freeze-drying
203 the polymerization mixture with no further purification. The yields were therefore nearly quantitative.
204 The PAA structures were assessed by ^{1}H-NMR (Figures S3-S5).

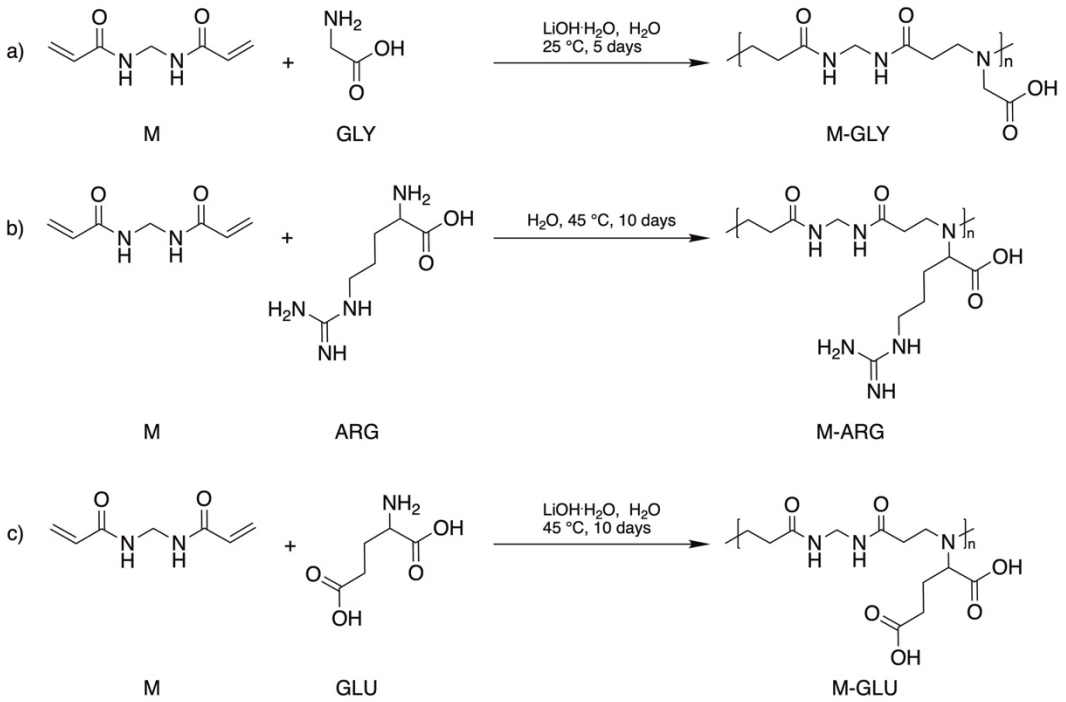

Scheme 1. Synthesis of M-GLY (**a**), M-ARG (**b**) and M-GLU (**c**).

205 *3.3 Interactions between MMT and PAAs*

206 Irrespective of the net average charge of their repeat units, all three polymers proved to form stable
207 interactions with MMT, as demonstrated by their ability to coagulate an opalescent 2% MMT water
208 suspension into a stable, dense, and milky suspension (Figure 3a). This is in line with previously
209 reported findings that adsorption of glycine and glutamic acid induces structural stress on
210 montmorillonite and widens its interlayer space [48]. The occurrence of strong interactions between
211 MMT and PAAs was confirmed by X-ray diffraction (XRD) spectroscopy, which was carried out on
212 both the solid MMT/PAA coagulates retrieved from the suspensions by freeze-drying and MMT
213 alone. The XRD spectra of MMT/PAAs (Figure 3b) revealed that the typical 001 XRD diffraction of
214 MMT at $2\Theta = 6.94°$ was shifted to lower angles for both M-GLY (4.96°) and M-ARG (4.84°),
215 indicating an increase of MMT interlamellar space (from 1.27 nm to 1.78 and 1.82 nm, for MMT, M-
216 GLY and M-ARG, respectively) hence the formation of an intercalated system [49]. It is apparent
217 that the interaction between MMT and M-GLU is even stronger than those in MMT/M-GLY and
218 MMT/M-ARG since the diagnostic MMT peak at $2\Theta = 6.94°$disappeared in the spectrum MMT/M-
219 GLU, indicating that this sample is exfoliated (Figure 3b). It is reasonable to assume that the different
220 morphologies observed depend on the specific distribution of ionic species of each PAA (Figure 1).
221 In fact, thanks to the presence of the protonated amino groups in the main chain and, in the case of
222 M-ARG, of the positively charged guanidinium pendants, all three PAAs can exchange with the
223 sodium cations present in the interlamellar spaces of the MMT giving intercalated systems. However,
224 the predominant negative charges present in the repeating units of M-GLU, due to the presence of a
225 second carboxyl group, can cause exfoliation of MMT due to electrostatic repulsion with the negative
226 charges present on the lamellae.

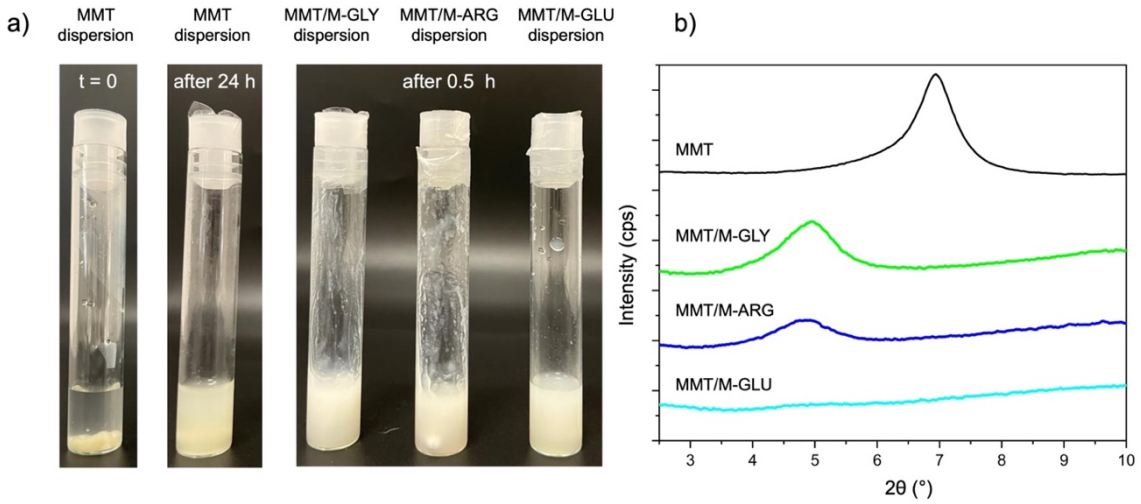

Figure 3. Pictures of MMT water dispersion at t = 0, after 24 h under stirring and MMT/M-GLY, MMT/M-ARG and MMT/M-GLU after 0.5 h mixing (**a**). XRD spectra of MMT, MMT/M-GLY, MMT/M-ARG and MMT/M-GLU (**b**).

227

3.4 Effect of MMT on the thermal and thermo-oxidative stability of PAAs

The TG and dTG thermograms in nitrogen and in air between 50 and 800 °C of M-GLY, M-ARG and M-GLU, and their MMT adducts (MMT/M-GLY, MMT/M-ARG and MMT/M-GLU) with a 1:7 MMT/PAA weight ratio, prepared as described in section 2.3, are shown in Figure 4. The related onset decomposition temperature at 10% weight loss, $T_{onset10\%}$, temperature at maximum weight loss rate, T_{max}, and residual mass fraction measured at 800 °C, RMF_{800}, are shown in Table 2.

As previously observed for other PAAs [35, 37], the thermal decomposition of PAA is driven by a complex multimodal mechanism that occurs with one major weight loss phase in nitrogen between 200 and 500 °C and two weight loss phases in air between 200 and 350 °C and 350 and 600 °C. The maximum weight losses are found in these temperature ranges. The TG curves in nitrogen were like those in air up to 350 °C, while, at higher temperatures, the two sets of curves diverged. More specifically, all PAAs showed a main decomposition phase in nitrogen starting at the $T_{onset10\%}$ (ranging from 137 and 150 °C, Table 2) with a T_{max} (236, 266 and 340 °C for M-GLY, M-ARG and M-GLU, respectively) and ended at around 350 °C. This thermal decomposition pattern did not change in the presence of MMT for M-GLY and M-ARG, as demonstrated by the TG curves in Figure 4a and $T_{onset10\%}$ and T_{max} values reported in Table 2. Conversely, in the case of M-GLU, MMT caused an anticipation of the thermal decomposition, as clearly visible in Figure 4a and comparing the $T_{onset10\%}$ and T_{max} values of M-GLU and MMT/M-GLU in Table 2. The RMF_{800} values were not affected by the presence of MMT.

In air, as observed in previous works [35, 37], PAAs exhibited two decomposition steps (Figure 4b) occurring with two maximum weight losses in between 236 - 263 °C (T_{max1}, Table 2) and 530 - 566 °C (T_{max2}). The first decomposition started in the $T_{onset10\%}$ range between 145 and 159 °C and ended at around 350 °C. The remaining residue oxidized completely between 350 and 600 °C, leaving a negligible RMF_{800} (1-2%). In air, the presence of MMT did not significantly affect PAA thermo-oxidative pattern, as visible in Figure 4b. $T_{onset10\%,}$ and T_{max1} and T_{max2} of PAAs were found to be comparable to those of MMT/PAAs. The only difference attributable to the presence of MMT was that the residue left at approximately 550°C oxidized more slowly between 550 and 800°C, as evidenced by comparison of the dTG curves. As a result, the RMF_{800} values of MMT/PAA were higher than those of PAAs (Table 2).

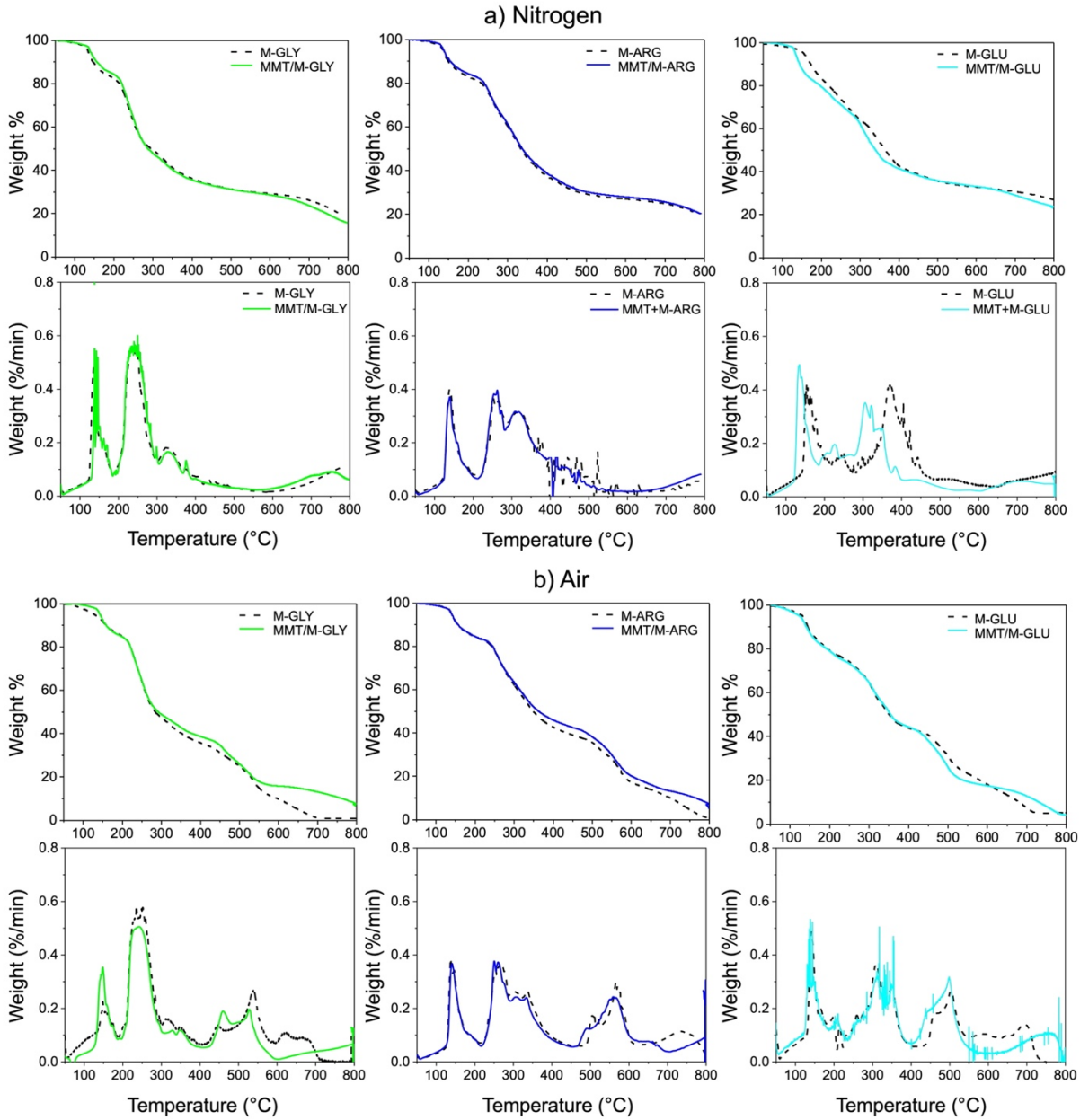

Figure 4. TG and dTG thermograms of PAAs and MMT/PAA adducts with a weight ratio of 1:7 in nitrogen (**a**) and air (**b**).

257

Table 2. Thermal data of PAAs in nitrogen and air by thermogravimetric analysis.

Sample	$T_{onset10\%}$ [a] (°C)	T_{max1} [b] (°C)	T_{max2}, T_{max3} [c] (°C)	RMF_{800} [d] (%)
		Nitrogen		
M-GLY	147	137, **236** [f]	-	19
M-ARG	149	139, **266** [f]	-	20
M-GLU	172	150, **340** [f]	-	24
MMT [e]	635	628	-	88
MMT/M-GLY	157	139, **242** [f]	-	19 [h]
MMT/M-ARG	155	142, **265** [f]	-	20 [h]

MMT/M-GLU	144	135, **306** [f)]	-	23 [h)]
		Air		
M-GLY	159	148, **236** [f)]	450, 540 [g)]	1
M-ARG	155	137, **263** [f)]	566 [g)]	1
M-GLU	145	149, **242** [f)]	458, 530 [g)]	2
MMT [e)]	642	111	626	88
MMT/M-GLY	159	149, **240** [f)]	459, 534 [g)]	7 [h)]
MMT/M-ARG	156	142, **257** [f)]	568 [g)]	5 [h)]
MMT/M-GLU	142	138, **352** [f)]	458, 532 [g)]	4 [h)]

[a)] Onset decomposition temperature at 10% weight loss. [b)] First temperature at maximum weight loss rate. [c)] Second and third temperature at maximum weight loss rate. [d)] Residual mass fraction at 800 °C. [e)] TG and dTG curves in Figure S6. [f)] T_{max} corresponds to the maximum weight loss in the 200 - 350 °C range (step 1). [g)] T_{max2} and T_{max3} correspond to the maximum weight losses in the 200 - 350 °C (step 2), and 350 - 600 °C (step 3) range, respectively. [h)] This value includes around 2% MMT residue. MMT/PAA composition: 1:7 weight ratio.

3.5 Morphological characterization of MMT/PAA-treated cotton fabrics

The morphology of COT/MMT/M-GLY, COT/MMT/M-ARG and COT/MMT/M-GLU were observed by Scanning Electron Microscopy (SEM) and compared to that of untreated cotton (Figure 5). It is apparent that, in the treated samples, the MMT/PAA coating created a continuous film that filled the gap between the cellulose fibers. Both MMT and PAAs appeared homogeneously dispersed on cotton surfaces, as revealed by the EDX elemental mapping shown in Figures 6-8 for COT/MMT/M-GLY, COT/MMT/M-ARG and COT/MMT/M-GLU, respectively, and Figures S7 for COT/MMT. Specifically, a continuous distribution was observed not only of carbon (C) and oxygen (O), present in the cotton matrix, but also of nitrogen (N), present only in the PAA coating, and of silicon (Si) and aluminum (Al) present only in MMT.

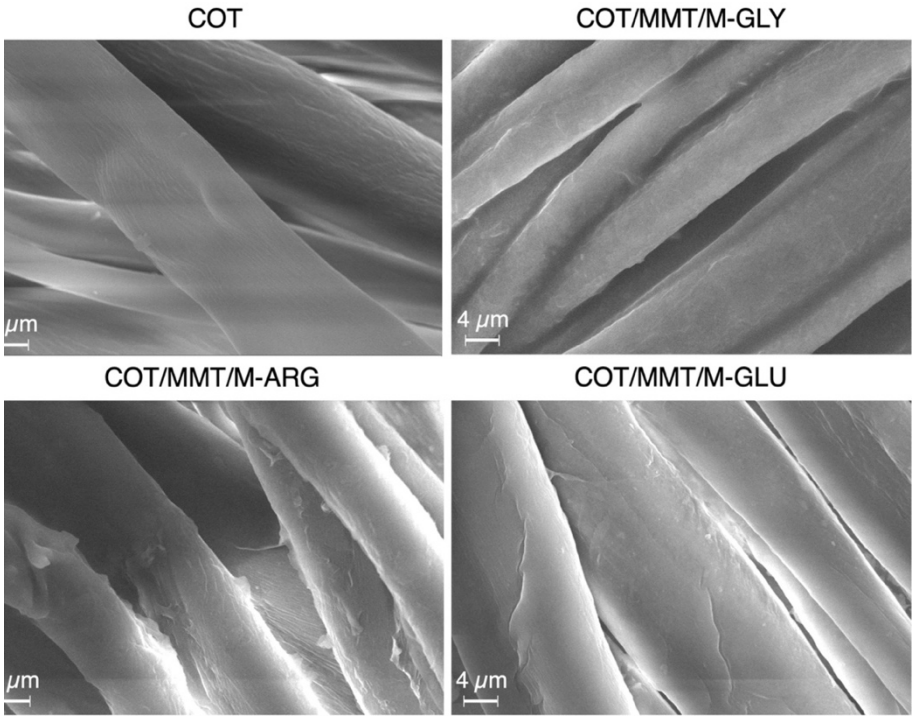

Figure 5. SEM micrographs (5000×) of untreated cotton (COT) and cotton fabrics treated with MMT (add-on: 2%) and M-GLY, M-ARG and M-GLU (add-on: 14%).

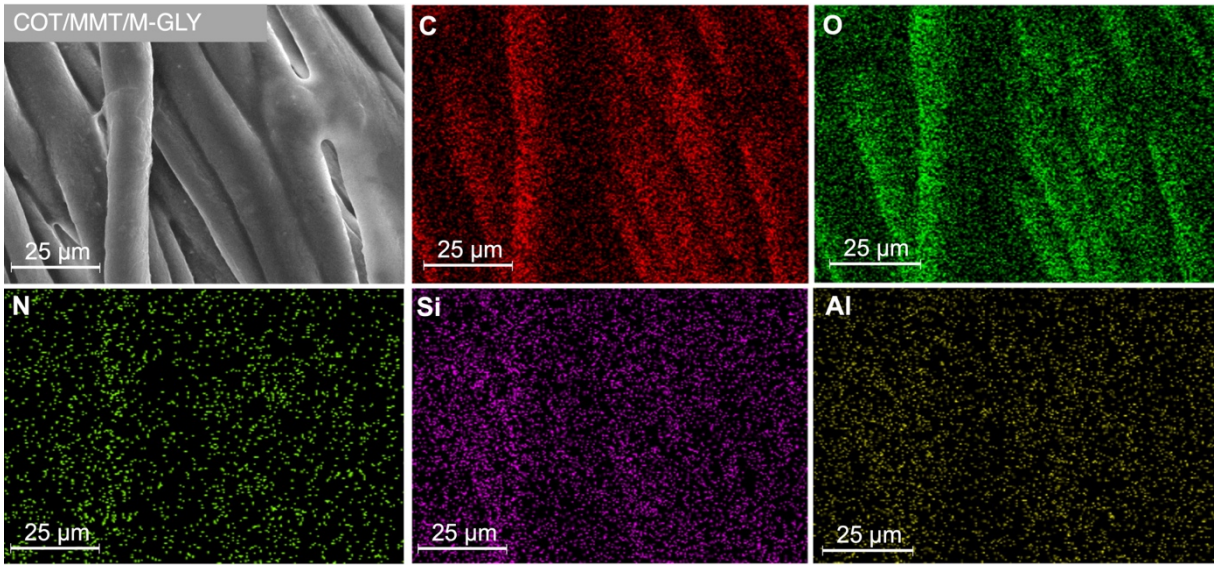

Figure 6. EDX analysis of COT/MMT/M-GLY (add-on: 2+14%).
Distribution of carbon (C), oxygen (O), nitrogen (N), silica (Si) and aluminum (Al) elements.

269

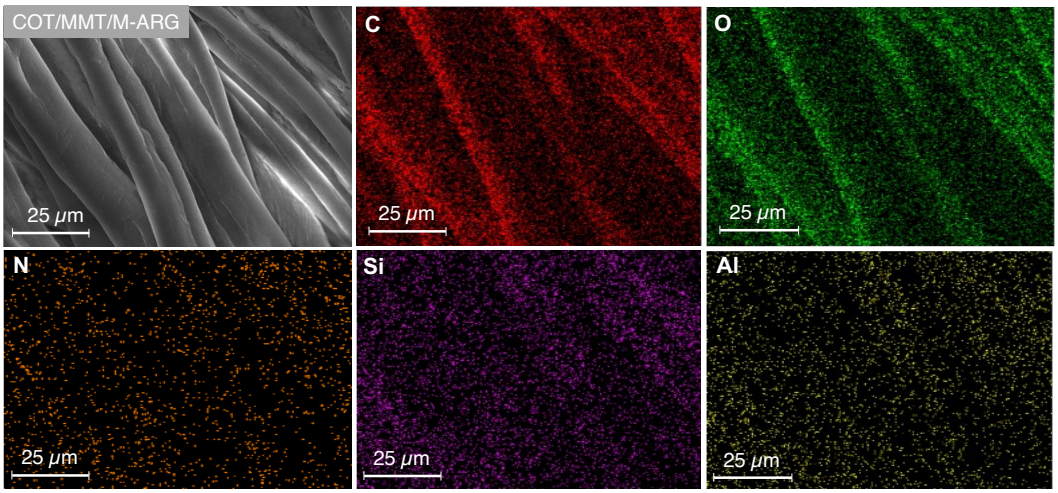

Figure 7. EDX analysis of COT/MMT/M-ARG (add-on: 2+14%).
Distribution of carbon (C), oxygen (O), nitrogen (N), silica (Si) and aluminum (Al) elements.

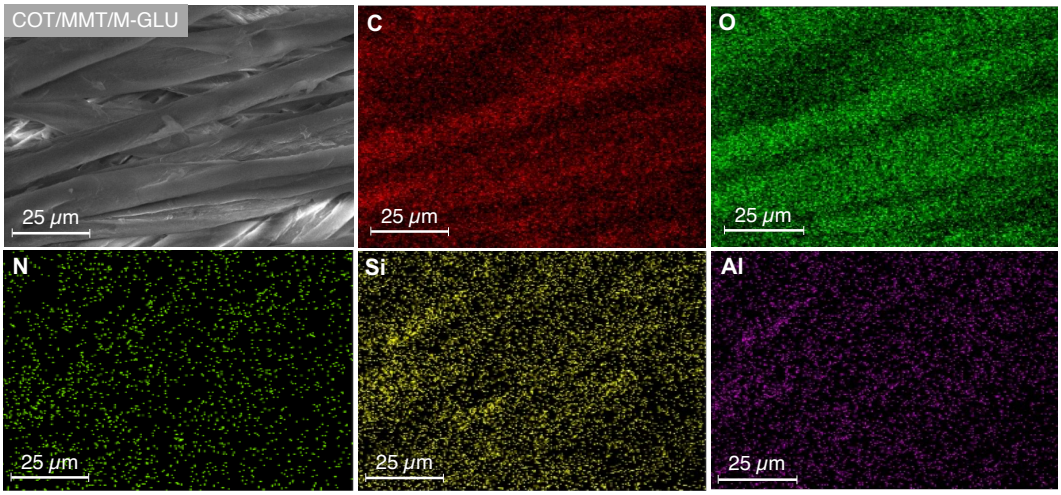

Figure 8. EDX analysis of COT/MMT/M-GLU (add-on: 2+14%).
Distribution of carbon (C), oxygen (O), nitrogen (N), silica (Si) and aluminum (Al) elements.

3.6 Whiteness of MMT/PAA-treated cotton fabrics

The white index (WI) values of COT/MMT/M-GLY, COT/MMT/M-ARG and COT/MMT/M-GLU were measured and compared to that of untreated cotton and cotton treated with MMT and PAAs alone (Figure 9). The presence of only 2% add-on MMT in COT/MMT caused a notable reduction in WI from approximately 82 down to 76, while 14% add-on PAAs caused a smaller reduction, although with qualification. In fact, in the case of COT/M-GLY and COT/M-ARG, the WI of cotton dropped to around 78 circa, while in COT/M-GLU to 75. The WI of COT/MMT/M-GLY did not significantly change with respect to that of COT/M-GLY, whereas it was further reduced to 75 in the case of COT/MMT/M-ARG and COT/MMT/M-GLU.

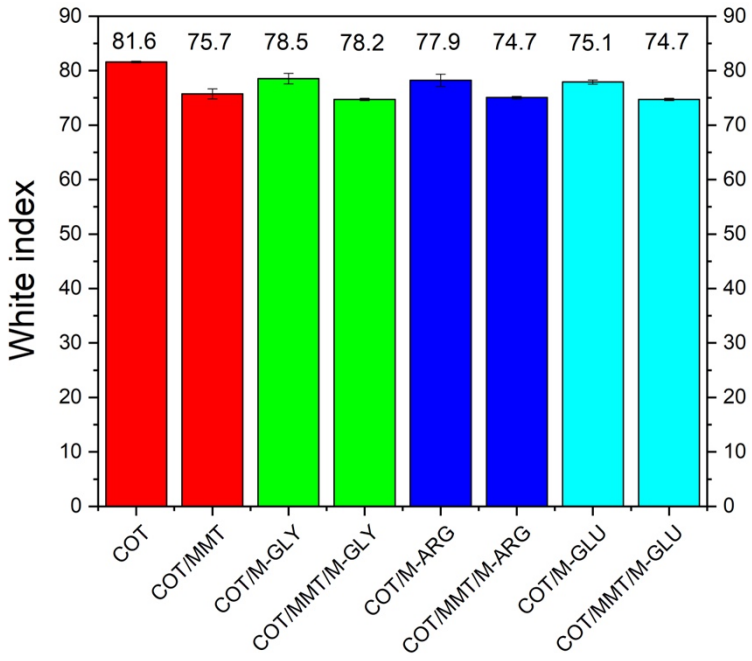

Figure 9. White index measurements of COT, COT/MMT, COT/PAA and COT/MMT/PAA. Add-ons: 2% MMT in COT/MMT; 14% PAA in COT/PAA samples; 2% MMT and 14% PAA in COT/MMT/PAA samples.

3.7 Mechanical properties of MMT/PAA-treated cotton fabrics

It has been previously observed that the hand of PAA-treated cotton fabrics changed significantly only at high PAA add-ons, namely above 20%, whereas for lower add-ons, they are rather soft and pleasant to the touch [50]. The present study confirmed this general behavior, since 14% PAA add-on did not significantly change the hand of the fabrics, while COT/MMT coatings with 2% MMT and COT/MMT/PAA (2% MMT + 14% PAA) made the cotton more rigid.

Furthermore, the effect of the PAA and the PAA/MMT nanocomposite coatings on the mechanical behavior of cotton textiles was studied by tensile tests and compared with that of a 2% MMT coating. The obtained stress-strain diagrams are shown in Figures 10a - 10c, while the maximum tensile strength values of all samples are shown in Figure 10d. The collected data are reported in Table S1. It is apparent that none of the polymer coating, either PAA or MMT/PAA nanocomposite coatings, significantly affected the tensile behavior of cotton since the stress-strain curves are very close to that of cotton. Only small differences (< 5%) in the maximum tensile strength values of the treated cotton samples were observed compared to untreated cotton, except for COT/M-ARG, in which the strength of cotton was increased by 12%, probably due to the significant cationic nature of M-ARG (Table 1), which favors the interaction with cellulose. A different effect was observed in COT/MMT, where the inorganic coating induced a slight increase in the maximum tensile strain, while maintaining the tensile strength almost unaffected.

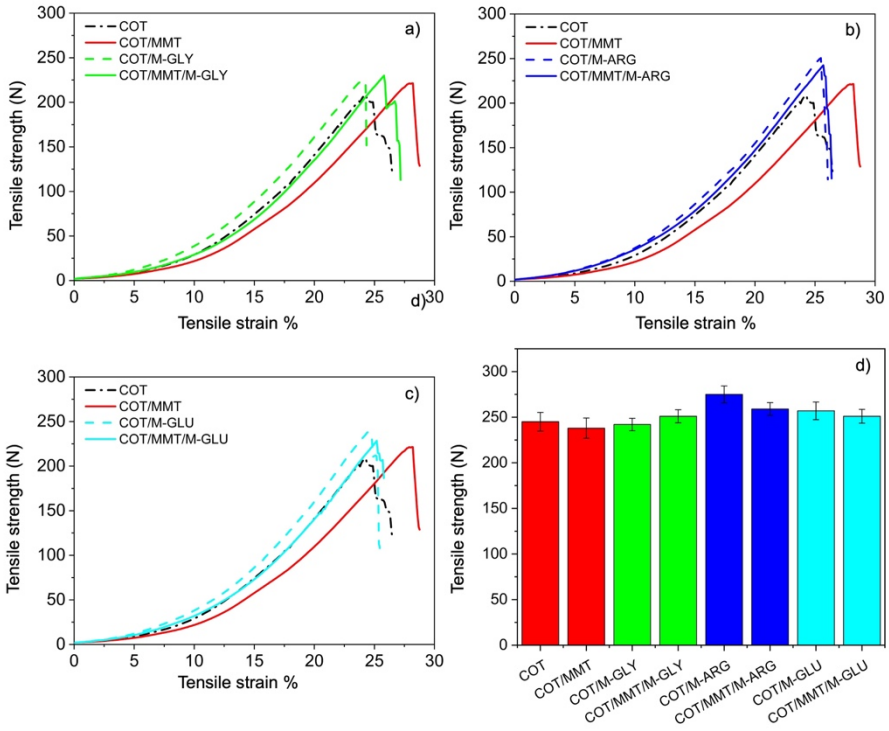

Figure 10. Tensile stress-strain diagrams of COT and COT/MMT in comparison with COT/M-GLY and COT/MMT/M-GLY (**a**); COT/M-ARG and COT/MMT/M-ARG (**b**); COT/M-GLU and COT/MMT/M-GLU (**c**); maximum tensile strengths of COT, COT/PAAs and COT/MMT/PAAs (**d**). Add-ons: 2% MMT in COT/MMT; 14% PAA in COT/PAA samples; 2% MMT and 12% PAA in COT/MMT/PAA samples.

3.8 Effect of MMT on the thermal stability of PAA-treated cotton fabrics

The thermal stability of COT/PAAs and COT/MMT/PAAs was investigated by TG analysis in nitrogen and air (Figures 11a and 11b) in the range 50-800 °C and the resulting thermograms compared with those of COT and COT/MMT. The observed $T_{onset10\%}$, T_{max} and RMF_{800} data are shown in Table 3. The effect of PAAs on the thermal and thermo-oxidative stability of cotton was as previously described for all the investigated PAAs [35, 37]. In nitrogen (Figure 11a), COT/PAA samples with 14% PAA add-on featured one single large weight loss, irrespective of the PAA considered, as did cotton. However, the PAA coatings induced a shift of $T_{onset10\%}$ and T_{max1} values to lower temperatures (Table 3), as well as a significant increase of the residual mass fractions above 350 °C. The replacement of 2% PAA with an equivalent amount of MMT induced only a slight increase in the thermal stability of COT/M-GLY and COT/M-GLU and a significant improvement of the thermal stability of COT/M-ARG, particularly above 350°C. In air (Figure 11b), the TG curve of untreated cotton showed two inflections, placed at 342 and 472 °C, and the RMF drops rapidly to 0% from 350 to 500 °C. As in nitrogen, the PAA coating induced a shift of the $T_{onset10\%}$ and T_{max1} values to lower temperatures, as well as an evident increase of the residual mass fraction above 350°C, while

the T_{max2} value remained almost unchanged. As in nitrogen, the replacement of 2% PAA with an equivalent amount of MMT induced only a slight increase in the thermal stability of COT/M-GLY and COT/M-GLU and a significant improvement of the thermal stability of COT/M-ARG, particularly above 350°C.

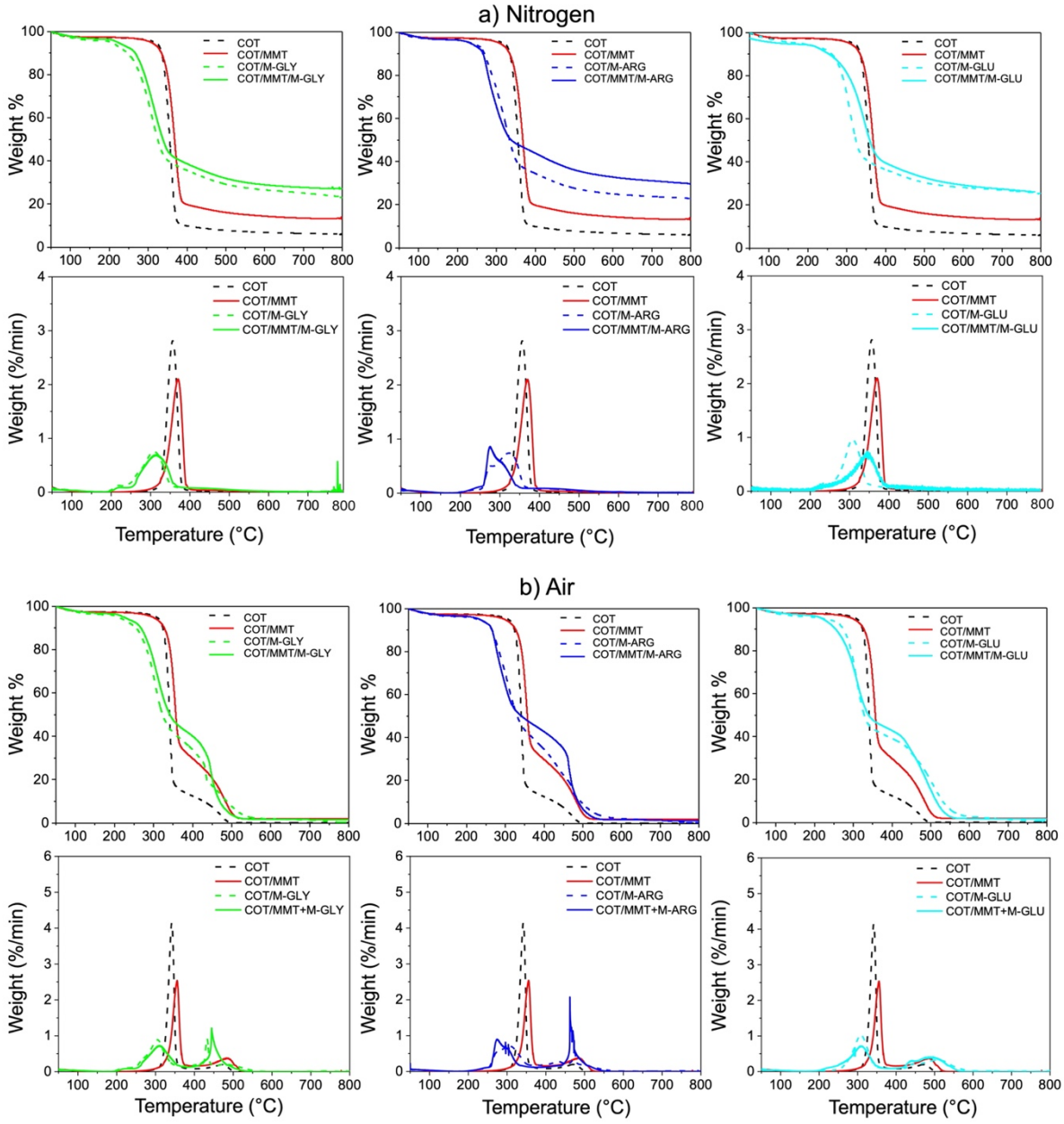

Figure 11. TG and dTG thermograms of COT, COT/MMT and COT/MMT/PAAs in nitrogen (**a**) and air (**b**). Add-ons: 2% MMT in COT/MMT; 14% PAA in COT/PAA samples; 2% MMT and 14% PAA in COT/MMT/PAA samples.

Table 3. Thermal data of COT/PAA and COT/MMT/PAA samples in nitrogen and air by thermogravimetric analysis.

Sample	Add-on [a] (%)	$T_{onset10\%}$ [b] (°C)	T_{max1} [c] (°C)	T_{max2}, T_{max3} [d] (°C)	RMF_{800} [e] (%)
Nitrogen					
COT	-	335	356	-	6
COT/M-GLY	14	247	310	-	23
COT/M-ARG	14	269	324	-	23
COT/M-GLU	14	262	309	-	23
COT/MMT	2	334	370	-	13 [e]
COT/MMT/M-GLY	2+12	267	314	-	27 [e]
COT/MMT/M-ARG	2+12	266	276	-	29 [e]
COT/MMT/M-GLU	2+12	254	345	-	28 [e]
Air					
COT	-	324	342	472	0
COT/M-GLY	14	256	304	433, 481	0
COT/M-ARG	14	266	305	434, 473	1
COT/M-GLU	14	274	308	446, 508	1
COT/MMT	2	327	353	487	2 [e]
COT/MMT/M-GLY	2+12	268	311	446	2 [e]
COT/MMT/M-ARG	2+12	266	276	466	2 [e]
COT/MMT/M-GLU	2+12	256	309	440, 492	2 [e]

[a] Add-on ± 0.5 %. [b] Onset decomposition temperature at 10% weight loss. [c] First temperature at maximum weight loss rate in the 300 - 400 °C range (step 1). [d] Second and third temperature at maximum weight loss rate in the 200 - 350 °C (step 2) and 350 - 600 °C (step 3) range, respectively). [e] Residual mass fraction at 800 °C. [f] This value includes around 2% MMT residue.

3.9 Combustion study of MMT/PAA-treated cotton fabrics

The aim of this work was to ascertain whether combining sodium montmorillonite, which produces during burning a silica coating which insulates and shields the underlying polymer, with intumescent PAA flame retardants, could give rise to a synergistic behavior that significantly improved the flame resistance of cotton. To demonstrate this assumption, the combustion behavior of COT/MMT/M-GLY, COT/MMT/M-ARG and COT/MMT/M-GLU was assessed by horizontal flame spread tests (HFSTs), vertical flame spread (VFSTs), limiting oxygen index (LOI) tests and oxygen-consumption cone calorimetry tests. The outcomes were compared with those of COT as well as of COT/M-GLY, COT/M-ARG, COT/M-GLU and COT/MMT, taken as reference formulations.

338 *3.9.1 Horizontal Flame Spread Tests*

339 Cotton fabrics treated with the MMT/PAA coatings were tested in horizontal configuration, applying
340 a flame for 3 s. Their flame retardant performances were assessed and compared with those of COT,
341 COT/MMT and COT/PAA fabrics used as benchmarks. Table 4 shows the meaningful data, including
342 add-ons, afterglow combustion time (A_t), extinguishment and RMF. Figure 12 shows snapshots taken
343 during combustion tests. As expected, when a flame was applied to an untreated cotton fabric, it
344 vigorously and completely burned, leaving <1% residue at the end of the test. The addition of 2%
345 add-on MMT did not allow to extinguish the flame but increased the RMF value to 17%. Conversely,
346 PAA coatings at 7% add-on enhanced the flame retardancy of cotton, suppressing the flame and
347 leaving high RMF. However, the COT/PAA specimens were affected by long-lasting afterglow,
348 which significantly reduced by replacing 2% PAA with an equivalent amount of MMT, while
349 maintaining substantially unchanged RMFs.
350

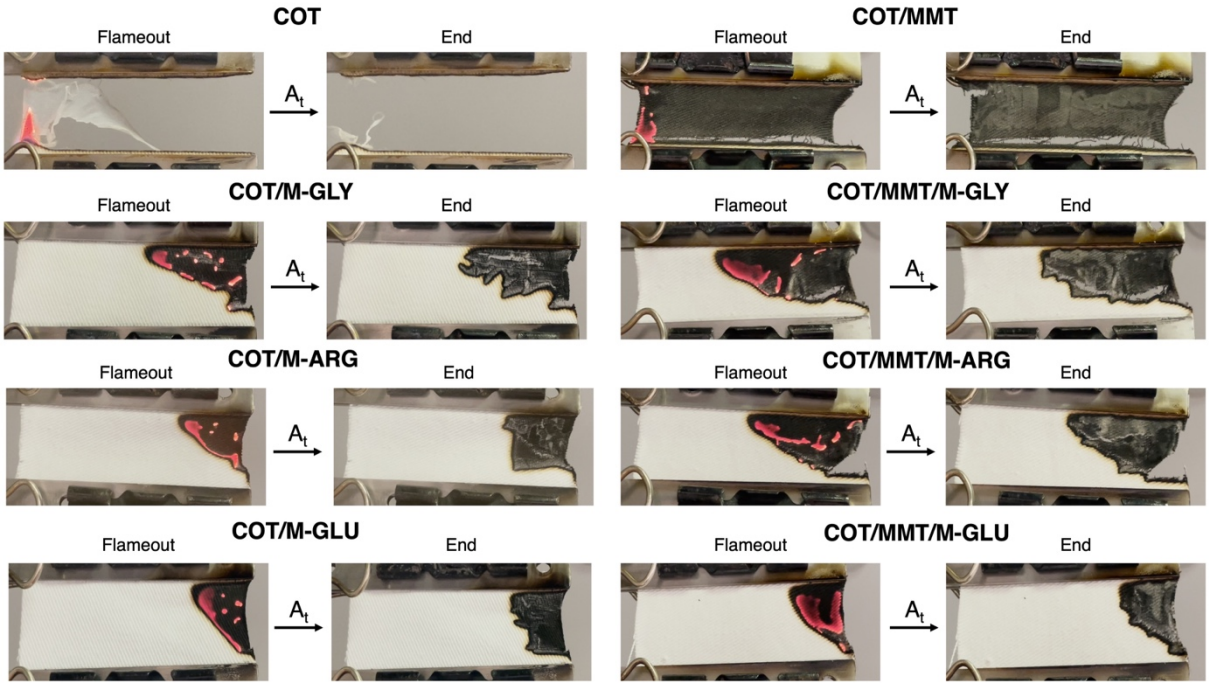

Figure 12. Snapshots of HFSTs carried out on COT, COT/MMT, COT/PAA and COT/MMT/PAA samples. Add-ons: 2% MMT in COT/MMT; 7% PAA in COT/PAA samples; 2% MMT and 5% PAA in COT/MMT/PAA samples. Flameout indicates when the flame disappears, and combustion proceeds only due to the afterglow; End means end of the combustion test.

Table 4. Combustion data of untreated cotton and MMT/PAA-treated cotton fabrics in HFSTs.

Sample	Add-on [a] (%)	Afterglow Time (s)	Extinguishment	RMF [b] (%)
COT	-	6 ± 1	NO	<1
COT/MMT	2	51 ± 3	NO	17 ± 3

COT/M-GLY	7	70 ± 14	YES	71 ± 1
COT/M-ARG	7	62 ± 2	YES	75 ± 7
COT/M-GLU	7	61 ± 9	YES	85 ± 4
COT/MMT/M-GLY	2 + 5	33 ± 1	YES	82 ± 13
COT/MMT/M-ARG	2 + 5	38 ± 1	YES	72 ± 2
COT/MMT/M-GLU	2 + 5	37 ± 1	YES	91 ± 7

[a)] Add-on ± 0.5 %. [b)] Residual mass fraction.

351

352 *3.9.2 Vertical Flame Spread and LOI tests*

353 The vertical configuration is notoriously more drastic than the horizontal one, due to the natural
354 upright direction of the flame, which widens the contact area between the sample and the flame.
355 Consequently, untreated cotton burned faster in VFSTs than in HFSTs, leaving no residue at the end
356 of the test (Figure 13). Cotton fabrics treated with the MMT/PAA coatings were tested in vertical
357 configuration, applying a flame for 2 s. Their flame retardant performances were assessed and
358 compared with those of COT, COT/MMT and COT/PAA fabrics used as benchmarks. Table 5 shows
359 the main combustion data, namely add-ons, total combustion time, extinguishment and RMF. Figure
360 13 shows some snapshots taken during combustion tests. Since in vertical configuration none of the
361 investigated PAAs extinguished the flame at 30% add-on [37], this add-on value was initially taken
362 as a reference in VFSTs carried out on COT/MMT/PAA coatings by replacing 2% add-on of PAA
363 with an equivalent amount of MMT. Notably, at a 2% add-on, MMT did not extinguish the flame,
364 although the final RMF was 12%, that is, higher than that left by cotton. All COT/MMT/PAA
365 specimens containing 2% MMT and 14% PAA add-ons did not ignite, exhibiting only slight thermo-
366 oxidation as revealed by the low combustion times (7 - 15 s) (Table 4) and the high RMF values,
367 which stood at 99% for all samples. The marked flame resistance of the COT/MMT/PAA samples
368 compared to that of cotton samples coated separately either with MMT or with each single PAA,
369 clearly demonstrates the emergence of a high synergy between the action of the MMT and PAAs in
370 the composite coatings.
371 To identify the minimum PAA add-on acting in synergy with 2% MMT, combustion tests were
372 carried out on samples containing PAA coatings with 11% and 8% add-ons. Among cotton specimens
373 treated with 2% MMT and 11% PAA add-on, both COT/MMT/M-GLY and COT/MMT/M-ARG
374 samples ignited, although they exhibited a different combustion resistance. MMT/M-GLY was indeed
375 not effective in stopping cotton burning, while MMT/M-ARG induced self-extinguishment of cotton,
376 although after a burning time as long as 234 s (Table 5 and Figure S8). This resulted in substantially
377 different RMF values (14% and 42% for COT/MMT/M-GLY and COT/MMT/M-ARG, respectively)
378 (Table 4). At the same add-on, the COT/MMT/M-GLU samples did not ignite and left 99% RMF

(Table 4). Further reducing PAA content to 8%, all samples ignited and only COT/MMT/M-GLU samples extinguished the flame, with an 82% RMF (Figure S9).

The synergism between PAA and MMT was further confirmed by LOI tests. Indeed, LOI values increased from 18% for untreated cotton, COT/MMT and COT/PAAs to 22.0%, 23.5% and 25.0% for COT/MMT/M-GLY, COT/MMT/M-ARG and COT/MMT/M-GLU, respectively. The minor differences observed among the effects of the composite coatings can reasonably be explained based on the different morphologies revealed by the XRD analyses (Figure 3b). In fact, while it has been demonstrated that the MMT/M-GLY and MMT/M-ARG adducts are intercalated systems, MMT/M-GLU proved to be an exfoliated system, therefore probably characterized by better barrier properties against oxygen and combustion gases [51].

Figure 13. Snapshots of VFSTs carried out on COT, COT/MMT and COT/MMT/PAA samples. Add-ons: 2% MMT in COT/MMT; 2% MMT and 14% PAA in COT/MMT/PAA samples.

Table 5. Combustion data of untreated cotton and MMT/PAA-treated cotton fabrics in VFSTs.

Sample	Add-on [a] (%)	Ignition	Combustion Time (s)	Extinguishment	RMF [b] (%)
COT	-	YES	27 ± 1	NO	<1
COT/MMT	2	YES	46 ± 1	NO	12 ± 2 [c]
COT/MMT/M-GLY	2+14	NO	7 ± 10	-	99 ± 0 [c]
COT/MMT/M-ARG	2+14	NO	15 ± 7	-	99 ± 0 [c]
COT/MMT/M-GLU	2+14	NO	10 ± 10	-	99 ± 1 [c]
COT/MMT/M-GLY	2+11	YES	138 ± 3	NO	14 ± 0 [c]
COT/MMT/M-ARG	2+11	YES	234 ± 64	YES	42 ± 10 [c]

COT/MMT/M-GLU	2+11	NO	10 ± 67	-	99 ± 0 [c)]
COT/MMT/M-GLY	2+8	YES	132 ± 23	NO	12 ± 2 [c)]
COT/MMT/M-ARG	2+8	YES	115 ± 8	NO	14 ± 0 [c)]
COT/MMT/M-GLU	2+8	YES	109 ± 66	YES	82 ± 2 [c)]

[a)] Add-on ± 0.5 %. [b)] Residual mass fraction.[c)] This value includes around 2% MMT residue.

391

392 *3.9.3 Oxygen-consumption cone calorimeter tests*

393 Cotton fabrics treated with the MMT/PAA coatings were subjected to an irradiative heat flux of 35
394 kW·m^{-2} using an oxygen-consumption cone calorimeter. Their behavior was compared with that of
395 plane cotton and PAA-treated cotton. The results, including combustion parameters such as TTI,
396 pHRR, THR and RMF are reported in Table 6; HRR curves are shown in Figure 14. Observing TTI
397 values and HRR curves in between 0 - 15 s time range, it is apparent that the presence of the PAA
398 coatings has sensitized cotton towards thermal decomposition. However, PAA-treatment induced a
399 decrease in the cotton pHRR by around 25% (22, 22 and 26% for M-GLY, M-ARG and M-GLU,
400 respectively, Table 6) and increased the RMFs by approximately 13% (12.8, 14.4 and 13.2 % for M-
401 GLY, M-ARG and M-GLU, respectively). MMT alone slightly reduced cotton pHRR (9%),
402 promoting a significant RMF (6.2%). The latter value demonstrated that MMT promotes cellulose
403 dehydration at the expense of depolymerization since the amount of clay is only 2%. The MMT/PAAs
404 combination decreased the pHRR of cotton by around 30%, and slightly reduced its THR.

405

406 **Table 6.** Combustion data of untreated cotton and MMT/PAA-treated cotton fabrics in oxygen-consumption cone
407 calorimeter tests.

Sample	**Add-on[a)] (%)**	**TTI (s)**	**pHRR (kW·m^{-2}) *(reduction, %)***	**THR (MJ·m^{-2})**	**RMF [b)] (%)**
COT	-	21 ± 3	125 ± 3	3.9 ± 0.1	0
COT/MMT	2	19 ± 1	114 ± 2 (*-9*)	4.0 ± 0.1	6.2 [c)] ± 2.8
COT/M-GLY	16	12 ± 3	97 ± 2 (*-22*)	4.0 ± 0.1	12.8 ± 0.4
COT/M-ARG	16	12 ± 2	97 ± 4 (*-22*)	3.7 ± 0.1	14.4 ± 2.1
COT/M-GLU	16	14 ± 2	92 ± 2 (*-26*)	3.9 ± 0.2	13.2 ± 2.3
COT/MMT/M-GLY	2+14	15 ± 1	87 ± 2 (*-30*)	3.6 ± 0.1	14.4 [c)] ± 2.5
COT/MMT/M-ARG	2+14	14 ± 0	86 ± 4 (*-29*)	3.6 ± 0.2	17.2 [c)] ± 2.8
COT/MMT/M-GLU	2+14	14 ± 2	91 ± 3 (*-27*)	3.7 ± 0.0	17.3 [c)] ± 3.9

[a)] Add-on ± 0.5 %. [b)] Residual mass fraction. [c)] This value includes around 2% MMT residue.

408

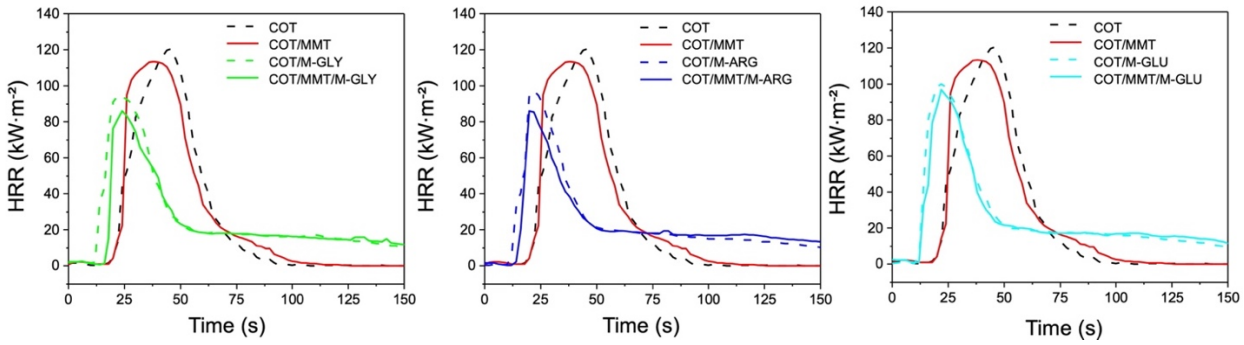

Figure 14. HRR curves of COT, COT/MMT, COT/PAAs and COT/MMT/PAAs. Add-ons: 2% MMT in COT/MMT; 2% MMT and 14% PAA in COT/MMT/PAA samples.

4. Conclusions

The α-amino acid-derived PAAs synthesized by the reaction of *N,N'*-methylenebisacrylamide with glycine (M-GLY), arginine (M-ARG) and glutamic acid (M-GLU) act as effective intumescent flame retardants for cotton in horizontal flame spread tests, although they fail to induce flame extinguishment in vertical flame spread tests. All three PAAs are amphoteric and at pH 4.0, at which PAAs are normally deposited on cotton, and present a different net charge per repeat unit, namely +1.02, +0.005 and -0.35 for M-ARG, M-GLY and M-GLU, respectively. Irrespective of the net charge, they were found to give rise to strong interactions in water with sodium montmorillonite, MMT, due to the presence of protonated tert-amine groups in the main chain, and protonated guanidine pendants in the case of M-ARG. XRD analysis of the MMT/PAA adducts prepared in water revealed that MMT was completely exfoliated in MMT/M-GLU and intercalated in the MMT/M-GLY and MMT/M-ARG. This experimental evidence formed the basis for investigating whether MMT/PAA nanocomposite coatings can act as synergistic flame retardants, combining the inherent intumescent behavior of PAAs with the barrier properties of MMT, which creates a silica film during combustion that stiffens the char and inhibits mass, oxygen, and heat transfer.

TG analyses in nitrogen and air of MMT/PAA composites with the same composition as in the protective coatings applied to cotton strips, showed that in both atmospheres the clay induced only a slight improvement in the thermal stability of PAAs. Not surprisingly, the same result was observed in the TG analyses of MMT/PAA-treated cotton textile.

The flame retardant effectiveness of the MMT/PAA nanocomposite coatings were investigated by horizontal- and vertical-flame spread tests as well as by oxygen-consumption cone calorimeter tests and compared with those of the corresponding PAA coatings. In HFSTs, MMT/PAA coatings proved to be almost equally effective than PAAs alone. In fact, they extinguished the flame with a shorter afterglow time but with a comparable RMF. In VFSTs, where all three PAAs failed to protect cotton even at add-ons >30%, all MMT/PAA coatings proved very efficient in inhibiting cotton ignition, but

with qualification. In the presence of 2% MMT add-on, the minimum add-on required to inhibit ignition was 14% M-GLY, 11% for M-ARG and 8% for M-GLU. In these conditions, the combustion times were 7 s, 234 s and 109 s, and the RMF value 99%, 42% and 82% for MMT/M-GLY, MMT/M-ARG and MMT/GLU, respectively. In addition, the synergism between MMT and PAAs was demonstrated by the increase of the LOI value of cotton from 18% to 22.0%, 23.5%, 25.0% for MMT/M-GLY, MMT/M-ARG and MMT/GLU, respectively. In oxygen-consumption cone calorimeter tests performed at a 35 kWm^{-2} heat flux, the effect of MMT/PAAs was found to be cooperative in reducing pHRR and THR and improving the RMF.

The results obtained in this work demonstrate that the interaction of MMT with the protonated amine groups of α-amino acid-derived PAAs induce the formation of even more substantial amounts of char than PAAs alone, in particular between 300 °C and 500 °C when PAAs undergo intumescence. The synergistic action between MMT and PAA can be ascribed to the well-known ability of MMT to stiffen and strengthen char in the combustion of nanocomposites, enhancing its effectiveness as a shield for heat and mass transfer, and oxygen diffusion. These findings let's envisage a high potential for PAA-based hybrid organic/inorganic formulations of flame retardant for cotton.

It should be observed that the washing durability of the MMT/PAA systems is low, due to the high solubility of α-amino acid derived PAAs in aqueous media. However, the results of this work could be transferred to PAA-grafted cotton, which represent the goal of this line of research [52].

Acknowledgments

The Authors thank the Italian Ministry for the University and Research, project PRIN2022 N° 202237JYZN, for financial support. Furthermore, they also thank D. Pezzini (Politecnico di Torino) and S. Vitali (Università degli Studi di Milano) for the SEM observations and XRD experiments, respectively.

References

1. J. Alongi, G. Malucelli, Cotton flame retardancy: state of the art and future perspectives, RSC Adv. 5 (2015) 24239-24263, https://doi.org/10.1039/C5RA01176K.
2. A.R. Horrocks. Flame retardant challenges for textiles and fibres: New chemistry versus innovatory solutions, Polym. Degrad. Stabil. 96 (2011) 377-392, https://doi.org/10.1016/j.polymdegradstab.2010.03.036
3. I. Van der Veen, J. De Boer, Phosphorus flame retardants: properties, production, environmental occurrence, toxicity and analysis, Chemosphere 88 (2012) 1119-1153, https://doi.org/10.1016/j.chemosphere.2012.03.067

4. S. Gaan, G. Sun, Effect of phosphorus and nitrogen on flame retardant cellulose: a study of phosphorus compounds, J. Anal. Appl. Pyrolysis. 2 (2007) 371-377, https://doi.org/10.1016/j.jaap.2006.09.010
5. C. Ling, L. Guo, Z. Wang, A review on the state of flame-retardant cotton fabric: mechanism and applications, Ind. Crops and Products 194 (2023) 116264, https://doi.org/10.1016/j.indcrop.2023.116264
6. H.C. Lee, S. Lee, Flame retardancy for cotton cellulose treated with H_3PO_3, J. Appl. Polym. Sci. 29 (2018) 46497, https://doi.org/10.1002/app.46497
7. C.Q. Yang, W. Wu, Combination of a hydroxy-functional organophosphorus oligomer and a multifunctional carboxylic acid as a flame retardant finishing system for cotton: part II. Formation of calcium salt during laundering, Fire Mater. 27 (2010) 239-251, https://doi.org/10.1002/fam.826
8. J. Alongi, A. Frache, G. Malucelli, G. Camino, Multi-component flame retardant coatings. In Handbook of Fire Resistant Textiles; Selcen Kilinc, F., Ed.; Woodhead Publishing: Cambridge, UK, 2013; Chapter 4, 68-93.
9. G. Malucelli, F. Carosio, J. Alongi, A. Fina, A. Frache, G. Camino, Materials engineering for surface-confined flame retardancy, Mater. Sci. Eng. R Rep. 84 (2014) 1-20, https://doi.org/10.1016/j.mser.2014.08.001
10. J. Livage, M. Henry, C. Sanchez, Sol-gel chemistry of transition metal oxides. Prog. Solid State Chem. 18 (1988) 259-341, https://doi.org/10.1016/0079-6786(88)90005-2
11. Y. Liu, C. Chou, The effect of silicon sources on the mechanism of phosphorus–silicon synergism of flame retardation of epoxy resins, Polym. Degrad. Stabil. 90 (2005) 515-522, https://doi.org/10.1016/j.polymdegradstab.2005.04.004
12. D. Yu, W. Liu, Y. Liu, Synthesis, thermal properties, and flame retardance of phosphorus- containing epoxy-silica hybrid resins, Polym. Compos. 31 (2010) 334-339, https://doi.org/10.1002/pc.20809
13. G. Malucelli, Sol-Gel and Layer-by-Layer Coatings for Flame-Retardant Cotton Fabrics: Recent Advances, Coatings 10 (2020) 333; https://doi.org/10.3390/coatings10040333
14. Q. Ji, X. Wang, Y. Zhang, Q. Kong, Y. Xi. Characterization of poly (ethylene terephthalate)/SiO_2 nanocomposites prepared by sol-gel method. Appl. Sci. Manuf. 40 (2009) 878-882, https://doi.org/10.1016/j.compositesa.2009.04.010
15. F. Carosio, A. Di Blasio, F. Cuttica, J. Alongi, A. Frache, G. Malucelli, Flame retardancy of polyester fabrics treated by spray-assisted layer-by-layer silica architectures, Ind. Eng. Chem. Res. 52 (2013) 9544-9550, https://doi.org/10.1021/ie4011244
16. Y.C. Li, J. Schulz, S. Mannen, C. Delhom, B. Condon, S.C. Chang, M. Zammarano, J.C. Grunlan, Flame retardant behavior of polyelectrolyte-clay thin film assemblies on cotton fabric, ACS Nano 4 (2010) 3325-3337, https://doi.org/10.1021/nn100467e
17. Z. Ur Rehman, S.-H. Huh, Z. Ullah, Y.-T. Pan, D.G. Churchill, B.H. Koo, LBL generated fire retardant nanocomposites on cotton fabric using cationized starch-clay-nanoparticles matrix, Carbohydr. Polym. 274 (2021) 118626, https://doi.org/10.1016/j.carbpol.2021.118626

505 18. K.M. Holder, R.J. Smith, J.C. Grunlan, A review of flame retardant nanocoatings prepared using layer-
506 by-layer assembly of polyelectrolytes, J. Mater. Sci 52 (2017) 12923-12959,
507 https://doi.org/10.1007/s10853-017-1390-1
508 19. J. Hao, M. Lewin, C.A. Wilkie, J. Wang, Additional evidence for the migration of clay upon heating
509 of clay–polypropylene nanocomposites from X-ray photoelectron spectroscopy (XPS), Polym.
510 Degrad. Stabil. 91 (2006) 2482-2485, https://doi.org/10.1016/j.polymdegradstab.2006.03.023
511 20. Y. Tang, M. Lewin, Maleated polypropylene OMMT nanocomposite: Annealing, structural changes,
512 exfoliated and migration, Polym. Degrad. Stabil. 92 (2007) 53-60,
513 https://doi.org/10.1016/j.polymdegradstab.2006.09.013
514 21. M. Lewin, Y. Tang, Oxidation-migration cycle in polypropylene-based nanocomposites,
515 Macromolecules 41 (2008) 13-17, https://doi.org/10.1021/ma702094e
516 22. A.B. Morgan, J.W. Gilman, An overview of flame retardancy of polymeric materials: application,
517 technology, and future directions, Fire Mater. 37 (2013) 259-279, https://doi.org/10.1002/fam.2128
518 23. X. He, W. Zhang, R. Yang, The characterization of DOPO/MMT nanocompound and its effect on
519 flame retardancy of epoxy resin. Composites: Part A 98 (2017) 124-135,
520 https://doi.org/10.1016/j.compositesa.2017.03.020
521 24. M. Zanetti, T. Kashiwagi, L. Falqui, G. Camino, Cone calorimeter combustion and gasification studies
522 of polymer layered silicate nanocomposites, Chem. Mater. 14 (2002) 881-887,
523 https://doi.org/10.1021/cm011236k
524 25. W. He, P. Song, B. Yu, Z. Fang, H. Wang, Flame retardant polymeric nanocomposites through the
525 combination of nanomaterials and conventional flame retardants, Prog. Mater. Sci. 14 (2020) 100687,
526 https://doi.org/10.1016/j.pmatsci.2020.100687
527 26. P. Kiliaris, C.D. Papaspyrides, Polymer/layered silicate (clay) nanocomposites: An overview of flame
528 retardancy, Prog. Polym. Sci. 35 (2010) 902-958, https://doi.org/10.1016/j.progpolymsci.2010.03.001
529 27. M. Kotal, A.K. Bhowmick, Polymer nanocomposites from modified clays: Recent advances and
530 challenges, Prog. Polym. Sci. 51 (2015) 127-187, https://doi.org/10.1016/j.progpolymsci.2015.10.001
531 28. M. Bartholmai, B. Schartel, Layered silicate polymer nanocomposites: new approach or illusion for
532 fire retardancy? Investigations of the potentials and the tasks using a model system, Polym. Adv.
533 Technol. 15 (2004) 355-364, https://doi.org/10.1002/pat.483
534 29. B. Schartel, Considerations regarding specific impacts of the principal fire retardancy mechanisms in
535 nanocomposites. In Flame Retardant Polymer Nanocomposites, Morgan A.B., Wilkie, C.A.; John
536 Wiley & Sons, Hoboken, New Jersey, USA, 2007, Chapter 5, 107-129.
537 30. M. Lewin, Flame retarding polymer nanocomposites: Synergism, cooperation, antagonism, Polym.
538 Degrad. Stabil. 96 (2011) 256-269, https://doi.org/10.1016/j.polymdegradstab.2010.12.006
539 31. L. Costes, F. Laoutid, S. Brohez, Ph. Dubois, Bio-based flame retardants: when nature meets fire
540 protection, Mater. Sci. Eng. R Rep. 117 (2017) 1-25, https://doi.org/10.1016/j.mser.2017.04.001

32. P. Ferruti, Poly(amidoamine)s: Past, Present, and Perspectives, J. Polym. Sci. Polym. Chem. 51 (2013) 2319-2353, https://doi.org/10.1002/pola.26632
33. F. Danusso, P. Ferruti, Synthesis of tertiary amine polymers, Polymer 11 (1970) 88-113, https://doi.org/10.1016/0032-3861(70)90029-7
34. B.D. Mather, K. Visvanathan, K.M. Miller, T.E. Long, Michael addition reactions in macromolecular design for emerging technologies, Prog. Polym. Sci. 31 (2006) 487-531, https://doi.org/10.1016/j.progpolymsci.2006.03.001
35. A. Manfredi, F. Carosio, P. Ferruti, E. Ranucci, J. Alongi, Linear polyamidoamines as novel biocompatible phosphorus-free surface-confined intumescent flame retardants for cotton fabrics, Polym. Degrad. Stabil. 151 (2018) 52-64, https://doi.org/10.1016/j.polymdegradstab.2018.02.020
36. J. Alongi, P. Ferruti, A. Manfredi, F. Carosio, Z. Feng, M. Hakkarainen, E. Ranucci, Superior flame retardancy of cotton by synergetic effect of cellulose-derived nano-graphene oxide carbon dots and disulphide-containing polyamidoamines, Polym. Degrad. Stabil. 169 (2019) 108993, https://doi.org/10.1016/j.polymdegradstab.2019.108993
37. A. Beduini, P. Ferruti, F. Carosio, E. Ranucci, J. Alongi, Polyamidoamines derived from natural α-amino acids as effective flame retardants for cotton, Polymers 13 (2021) 3714, https://doi.org/10.3390/polym13213714
38. A. Beduini, F. Carosio, P. Ferruti, E. Ranucci, J. Alongi, Sulfur-based copolymeric polyamidoamines as efficient flame-retardants for cotton, Polymers 11 (2019) 1904, https://doi.org/10.3390/polym11111904
39. N. Mauro, F. Chiellini, C. Bartoli, M. Gazzarri, M. Laus, D. Antonioli, P. Griffiths, A. Manfredi, E. Ranucci, P. Ferruti, RGD-mimic polyamidoamine–montmorillonite composites with tunable stiffness as scaffolds for bone tissue-engineering applications, J. Tissue Eng. Regen. Med. 11 (2017) 2164, https://doi.org/10.1002/term.2115
40. P. Ferruti, N. Mauro, L. Falciola, V. Pifferi, C. Bartoli, M. Gazzarri, F. Chiellini, E. Ranucci, Amphoteric, prevailingly cationic L-arginine polymers of poly(amidoamino acid) structure: synthesis, acid/base properties and preliminary cytocompatibility and cell-permeating characterizations. Macromol. Biosci. 14 (2014) 390-400, , https://doi.org/10.1002/mabi.201300387
41. ISO 3795. Road vehicles, and tractors and machinery for agriculture and forestry - Determination of burning behaviour of interior materials; International Organization for Standardization: Geneva, Switzerland, 2019.
42. ISO 15025. Protective clothing - Protection against flame - Method of test for limited flame spread; International Organization for Standardization: Geneva, Switzerland, 2016.
43. ISO 4589. Plastics - Determination of burning behaviour by oxygen index - Part 1: General requirements; International Organization for Standardization: Geneva, Switzerland, 2017.

576 44. J. Tata, J. Alongi, F. Carosio, A. Frache, Optimization of the procedure to burn textile fabrics by cone
577 calorimeter: Part I. Combustion behavior of polyester, Fire Mater. 35 (2011) 397-409,
578 https://doi.org/10.1002/fam.1061
579 45. ISO 5660. Fire Test. Reaction to Fire, Rate of Heat Release - Cone Calorimeter Method; International
580 Organization for Standardization: Geneva, Switzerland, 2002.
581 46. ISO 2469. Paper, board and pulps. Measurement of diffuse radiance factor (diffuse reflectance factor);
582 International Organization for Standardization: Geneva, Switzerland, 2014.
583 47. ISO 13934-1. Textile - Tensile properties of fabrics. Part 1: Determination of maximum force and
584 elongation at maximum force using the strip method; International Organization for Standardization:
585 Geneva, Switzerland, 2013.
586 48. J. Nkoh Nkoh, Z. Hong, H. Lu, J. Li, R. Xu, Adsorption of amino acids by montmorillonite and
587 gibbsite: Adsorption isotherms and spectroscopic analysis, Appl. Clay Sci. 219 (2022) 106437,
588 https://doi.org/10.1016/j.clay.2022.106437
589 49. S.S Ray, M. Okamoto, Polymer/layered silicate nanocomposites: a review from preparation to
590 processing. Prog. Polym. Sci. 28 (2003) 1539-1641,
591 https://doi.org/10.1016/j.progpolymsci.2003.08.002
592 50. J. Alongi, R. Aad, P. Ferruti, E. Ranucci, Enhancing the flame resistance of cotton by exploiting the
593 interaction between calcium chloride and an aspartic acid-derived polyamidoamine. Cellulose 31
594 (2024) 623-642, https://doi.org/10.1007/s10570-023-05599-6
595 51. T.T. Zhu, C.H. Zhou, F. Bwalya Kabwe, Q.Q. Wu, C.S. Li, J.R. Zhang, Exfoliation of montmorillonite
596 and related properties of clay/polymer nanocomposites. Appl. Clay Sci. 169 (2019) 48-66,
597 https://doi.org/10.1016/j.clay.2018.12.006
598 52. A. Beduini, F. Porta, S. Nebbia, F. Carosio, E. Ranucci, P. Ferruti, J. Alongi J Durable, washing
599 resistant flame-retardant finishing for cotton fabrics by covalent grafting of α-amino acid-derived
600 polyamidoamines. Proceedings of the Milan Polymer Days Congress, 19-21 June 2022, Milan, Italy,
601 p. 7, ISBN 978-88-3623-096-9.